



Approach to Increase a Capturing Distance of Emissions in Industrial Ventilation

S.Y. Spotar^{1,*}, I.A. Chokhar²

¹Nazarbayev University, 53 Kabanbay Batyr Ave., Astana, 010000, Kazakhstan

²Institute of Thermophysics, 1 Lavrentiev Ave., Novosibirsk, 630000, Russia

*Corresponding author. Email address: sergey.spotar@nu.edu.kz

Abstract

Ventilation is important for controlling gaseous contaminant levels in workplaces, but the emissions capture distance of conventional intake hoods is limited. The vortex suction device (VSD) aims to elongate the intake flow region of local ventilation systems by exploiting the shielding features of specifically organized peripheral swirling jets. Herein, numerical CFD modeling and laser Doppler anemometry were used to investigate the confinement of intake flow by the buffer-recirculating cell shield generated from peripheral outflowing swirling jets. The measured velocity profiles yielded approximately a doubling of the intake capture distance by using the VSD equipped with a diffuser with a 90° opening angle. Potential applications for local ventilation tasks are discussed.

Keywords: Local ventilation; vortex suction device; CFD-modelling; laser Doppler anemometry.

1. Introduction

The concept of local ventilation lies in capturing contaminated air in the vicinity of the origin of hazardous emissions. Quite often, the configuration of the extraction flow induced by a conventional ventilation hood, may not adequately comply with the task requirements, especially when the intake hood aperture is not positioned sufficiently close to the emission source owing to the specifics of the technological process, for example, when the electrical arc welds a seam between sizeable parts. To address the above problem, the use of an adequate peripheral swirling flow has been proposed (Spotar et al., 1995).

The present study targets modeling and non-intrusive diagnosing of the velocity field in the intake flow when it is fenced by the peripheral swirled jets originating from the modified vortex suction device. In particular, the authors are interested in the details of the generation of the peripheral meridional recirculating cell to ensure the shielding effect, and hence, the elongation of the near-axis entrapping flow.

2. State of the art

Shtern and Hussain (Shtern & Hussain, 1996) analyzed a spacing configuration of the flow structure created by swirling jets at a far-field region with respect to the jet source through the reduction



of the Navier–Stokes equations to ordinary differential equations. They revealed that the angle of the jet propagation depends on the swirl parameter. However, they did not propose the design of the jet generator and carried out the relevant experiments. The application of a swirling flow generated by a rotating swirled (Lim, Lee, & Lee, 2011) or by the peripheral air outflow passing through a system of fixed vanes and declining radially outwards by the profiled diffuser (Spotar & Sorokin, 2010) yields the effect focusing of the intake stream, however, optimization of the apparatus for industrial needs requires a further understanding of the overall flow structure and the role key design parameters. For example, the use of only a single tangential inlet and the 90° opening diffuser allows simplifying the design of the apparatus (Chokhar &

Filippov, 2021). It is worth noting the substantial distinction between considered here the approach and apparatus with the employment of tornado-like vortex flow, in the last the interaction of the swirled flow with a lower-positioned horizontal surface is crucial for the desirable flow pattern generation (Perot & Pavlovich, 2010), (Wan, Feng, & Liu, 2010).

3. Materials and Methods

3.1. Vortex suction device (VSD) unit

Figure 1 shows the laboratory VSD model used in this study. In contrast to the original VSD with a vane-type vortex generator (Spotar et al., 1995; Spotar, 2004), the employed VSD comprises a small-size model with a single tangential swirl generator.

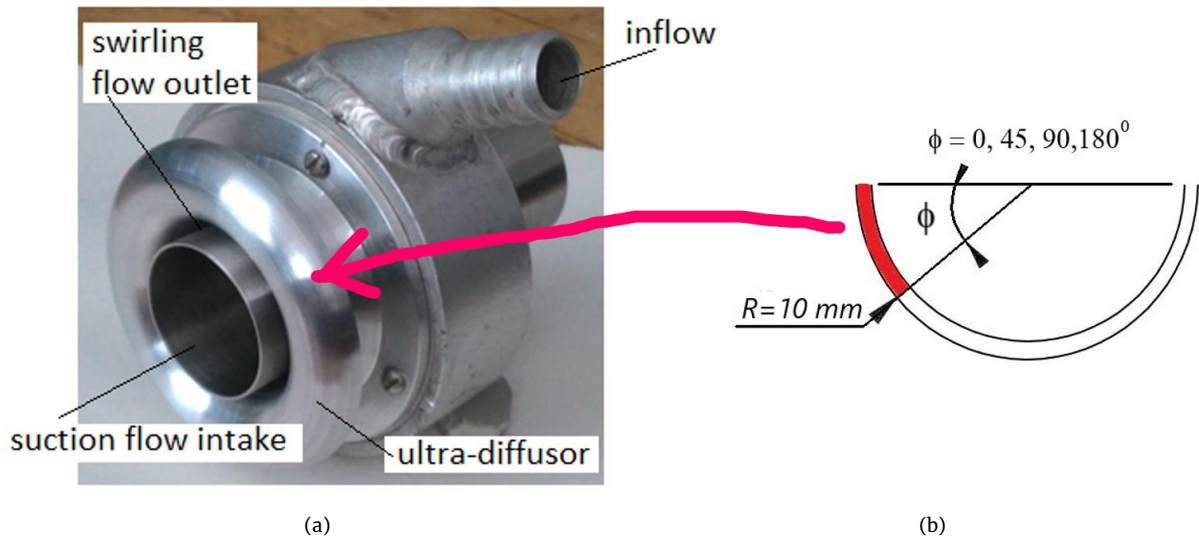


Figure 1. (a) Assembled vortex suction device (VSD), (b) design schematic of the diffuser.

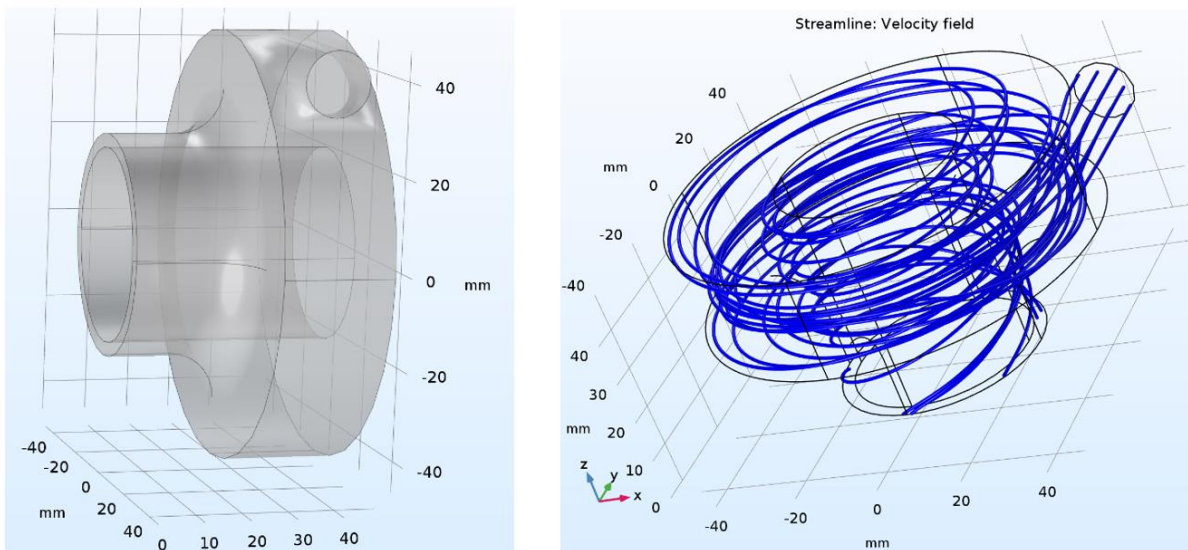


Figure 2. (a) Body of the swirl flow generator, and (b) simulated flow streamlines.

This VSD apparatus was designed such that the space dimensions of the created flow should comply with the range of measurements of the used laser velocimeter tool. The VSD apparatus operates two separated flows: a central cylindrical duct serves as a conduit for the intake flow, whereas the passage for the peripheral stream consists of a vortex chamber with a single tangential inlet 14 mm in diameter, a convergent cone section, and a 3-mm-wide annular outlet conjugated with the profiled diffuser. The interior of the unit assembly is shown in Figure 2(a). The suction intake aperture of this VSD model was 40 mm in diameter, and the curvature of the profiled diffuser was 10 mm.

3.2. Experimental setup

The velocities in the complex 3-D flow field generated VSD were investigated using the laser doppler anemometer LAD-06C, developed at the Institute of Thermophysics. The measuring setup consisted of the two-component LDA with an adaptive time selection of orthogonal channels and a 3-component coordinate-positioning device with a running accuracy of 0.0125 mm. The aerosol formed at re-condensation of glycerin vapors was used as a source of light-scattering particles (the average diameter of tracers was $1 \pm 0.1 \mu\text{m}$). In this study, the angular momentum of the peripheral flow was implicitly represented here by the swirl angle of $\approx 68^\circ$, and mass flow rates throughout the VSD were kept fixed as $4.6 \times 10^{-3} \text{ kg s}^{-1}$ and $3.95 \times 10^{-3} \text{ kg s}^{-1}$ for the suction stream and peripheral shielding flow, accordingly.

The key function of the profiled diffuser in this VSD is to decline outwards the swirling jet using the Coanda effect, the reported here results were obtained for the employed diffusers with 45° , 90° , and 180° opening angles (Figure 1a).

3.3. CFD simulation

The CFD package from COMSOL Multiphysics® v.5.6 software has been used in the simulation. The CFD's algorithm implements a numerical solution of the Reynolds-averaged Navier–Stokes equations.

Modeling has been carried out in 2 stages: initially, a 3-dimensional flow field has been obtained separately for the interior of the vortex generator formed by the peripheral conduit of the VSD (Figure 2a). This first auxiliary stage was necessary to determine the ratio of the tangential to the axial velocity of the peripheral swirling jet produced by the VSD at the outlet of the apparatus. The results of the simulation revealed that a circumferential distribution of the velocity magnitude at the chamber annular outlet flow is not completely uniform and exhibits $\pm 5\%$ circumferential variation of velocity due to using of the single tangential entrance for the peripheral stream. These averaged values of the axial and tangential velocity values obtained under 3-D modeling of the interior flow were used in the second

stage for setting the boundary conditions for the swirling annular jet generated by the device at its outlet. To reduce the bulk of numerical calculations, 2-D axisymmetric flow modeling was used to investigate the external flow structure generated by the VSD. A virtual sphere with a diameter of 500 mm and atmospheric pressure $p = 0$ (gauge pressure) as the boundary condition was defined as the modeling space beyond which the impact from the surroundings on the VSD operation can be neglected. (In the preliminary trials, the modeling spaces of 1600 mm and 800 mm diameter were tested; however, these extensions yielded essentially the same information on the operation of the VSD). ‘Extremely Fine’ mesh with approximately 100,000 elements (mostly triangular) was typically involved in the 2-D simulation procedure, and approximately 10 – 15 min was required to achieve solution convergence. The assumption of the 2-D axisymmetric generated flow configuration and the absence of drafts from the surrounding undoubtedly idealized reality but enhanced the capacity to analyze the number of potential design versions of the VSD. In this study, the CFD software was used as a preliminary search and exploratory tool for predicting the configuration of the focused intake flow generated by the VSD when varying its key design parameter. This is achieved by the specification of the design angle of the diffuser conjugated extension with the annular outlet of the swirling flow (Figure 1b). It is appropriate to indicate at least three factors that cause some disagreement between the model and experiments (as observed in the below-reported results):

1. Uncertainty of the available different turbulence models on the accurate prediction of the separation of the swirling jet from the diffuser, and hence the angle of the jet direction of propagation.
2. A non-symmetry of the real 3-D flow generated by the tested VSD model.
3. Uncertainties with the setting of boundary conditions, including the impact of uncontrolled (although weak) draft streams from the surrounding.

4. Results and Discussion

Simulation CFD results with different configurations of the flow generated by the VSD apparatuses are shown in Figure 3, which represents the velocity magnitude-controlled streamlines yielded by the VSD equipped with diffusers of 45° , 90° , and 180° ‘opening’ designed angles. A significant effect of the diffuser design opening angle on the resulting flow field can be observed; namely, the outflowing swirling jet creates a potential shielding effect, although it acts implicitly by the generation of the secondary recirculating cell positioned between the intake flow and the outlet jet flow. The VSD equipped with a 45° diffuser (Figure 3a) yielded significant confinement of the intake flow. However, note that in this case, the recirculating cell

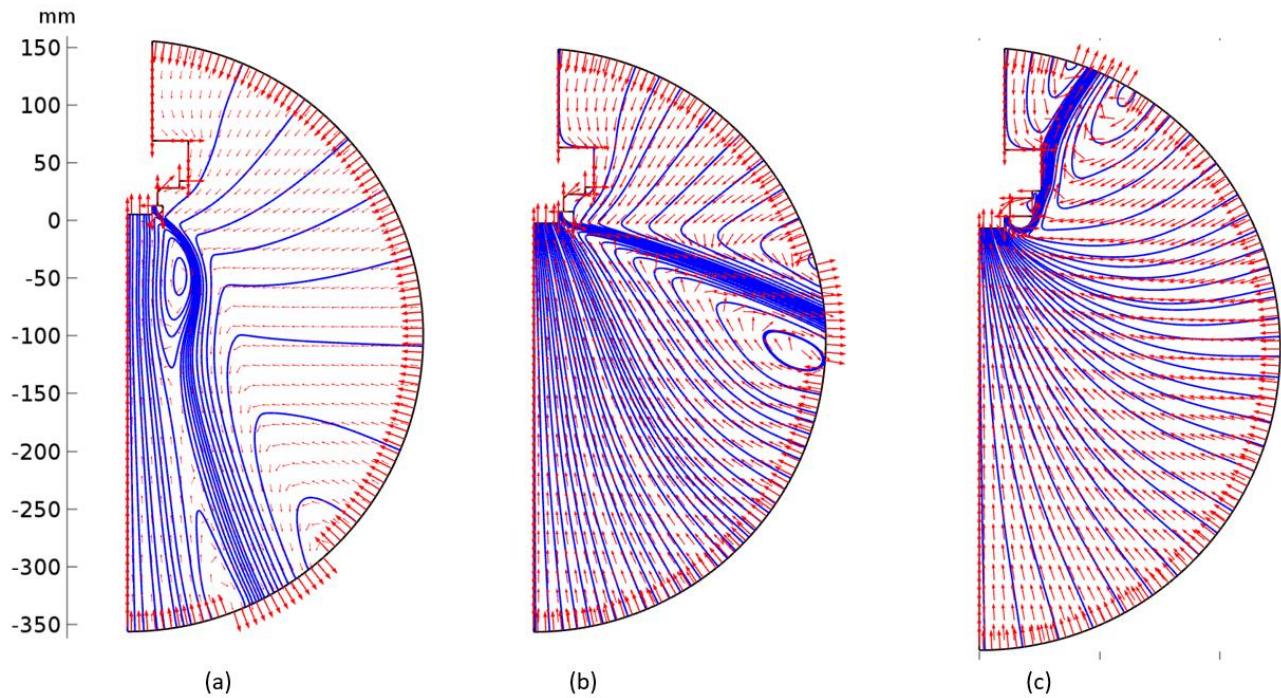


Figure 3. Impact of the diffuser design angle on the configuration of the flow induced by the VSD: (a) $\phi = 45^\circ$, (b) $\phi = 90^\circ$ and (c) $\phi = 180^\circ$.

separated the suction, and the outflowing in the opposite direction jet is quite narrow and characterized by higher velocity values when compared with separating buffer zones for 90° and 180° diffusers (Figure 3 b and c).

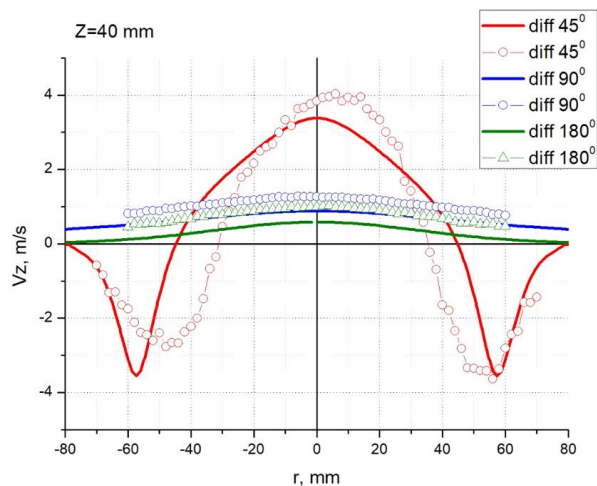


Figure 4. Radial distribution of the axial velocity in the intake flow generated by the VSD with different diffusers. Symbols – experiments, lines – calculated with CFD.

The experimental results of the LDA non-intrusive diagnostics of the flow velocity fields (Figures 4 – 7)

were used to verify the confinement and elongation of the intake flow.

The data were obtained by traversing the LDA's point-like measuring volume across and along the intake flow generated by the VSD under variation of the diffusers with 45° , 90° , and 180° opening angles.

The experimental velocity profiles of the axial velocity along with the CFD calculated results at $z = 40$ mm from the VSD intake aperture are shown in Figure 4. Although the experimental values of the measured velocities in the intake stream are somewhat higher than the predicted values calculated from the model, the experimental profile behavior complies with the calculated profiles and corresponds to the flow configuration shown in Figure 3.

The experimental velocity profiles of the tangential velocity along with the calculated results of CFD at the same distance of $z = 40$ mm from the VSD are shown in Figure 5. These data also agree well with the flow configuration provided in Figure 3. Additionally, it can be observed that the intake flow for the VSD equipped with 90° and 180° is practically non-swirl, whereas the intake stream for the VSD with a 45° diffuser at one orifice diameter distance ($z/d = 1$) possesses the same scale of the tangential velocity as the axial velocity component. The streamline's structure obtained by the CFD model allows the latest particular to be related to

the transport of the angular momentum by the recirculating cell from the outflowing swirling jet directed down and positioned close to the near-axis region.

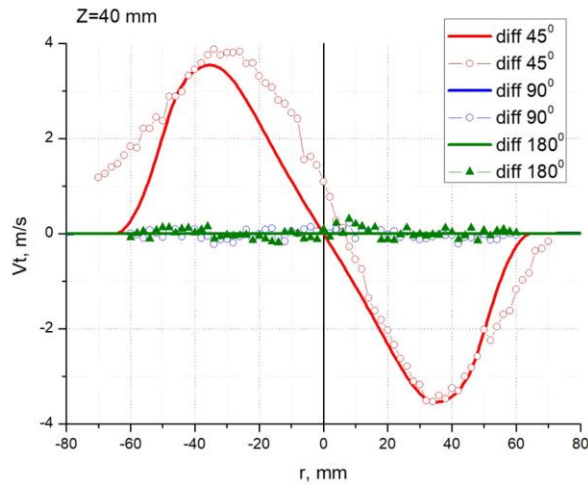


Figure 5. Radial distribution of the tangential velocity in the intake flow generated by the VSD with different diffusers. Symbols – experiments, lines – calculated with CFD.

Conventional ventilation hoods experience a limited distance range for capturing contaminated air. The velocity of the extraction flow in the vicinity of the hood is nearly inversely proportional to the squared distance from the entrance (an unfocused intake flow provided by a point sink flow model). The VSD apparatus, owing to the shielding effect, reduces the lowering of the value intake axial velocity at a given distance from the inflow aperture.

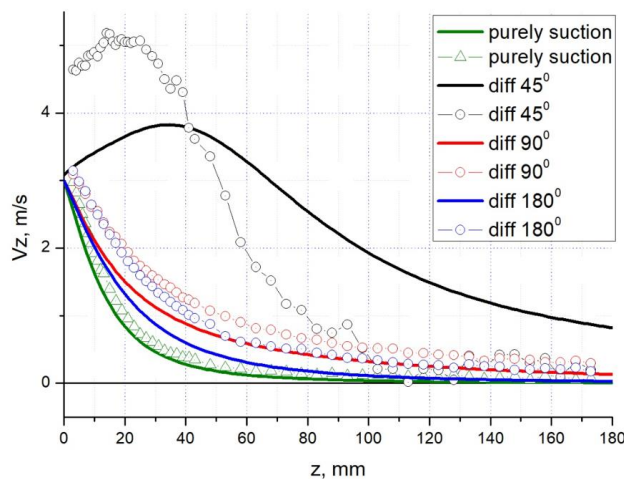


Figure 6. Axial distribution of the V_z -velocity component generated by the VSD with different diffusers. Symbols – experiments, lines – calculated with CFD.

This potential is demonstrated in Figure 6, where the case of purely suction (the peripheral flow is off) is included. The axial velocity decay curve for the VSD with 90° and 180° diffusers exhibits a gradual decay behavior like that of pure suction, but the corresponding velocity profiles are positioned higher.

With respect to the experimental and calculated velocity profiles $V_z = V_z(z)$ for the VSD with a 45° diffuser, these profiles are characterized by even higher values of the velocity compared with the pure suction flow; however, the maximum experimental value of the velocity is positioned not at the intake flow entrance but at $z/d \approx 0.5$. Here, the corresponding calculated curve $V_z = V_z(z)$ yields the maximum velocity, but at $z/d \approx 1$, and the calculated profile deviates from the experimental profile. The continuity equation assessing the position of the maximum velocity predicts the corresponding rise of the radial component of velocity that is directed outwards to feed the recirculating cell.

In accordance with the results presented above, it is important to understand whether the focused flow presented by the 'promising' intake streamlines, shown in Figure 4a for the VSD with a 45° diffuser, might be used for the convective transport of the captured contaminated air. However, 'an unfavorable' result should be noticed which is presented in Figure 7, where the radial profiles of the kinetic energy of turbulence k are given at $z/d = 0.25$.

The experimental values of the kinetic energy of turbulence were processed from three fluctuating velocities as follows:

$$k = \frac{1}{2} (\overline{V_z'^2} + \overline{V_t'^2} + \overline{V_r'^2})$$

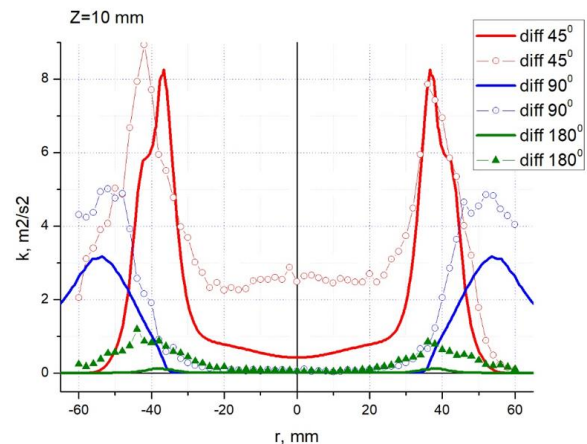


Figure 7. Radial distribution of the kinetic energy of turbulence in the intake flow generated by the VSD with different diffusers. Symbols – experiments, lines – calculated with CFD.

Analysis of the data presented in Figure 7 allows us to refer to the pure suction flow and intake streams provided by the VSD with 90° and 180° diffusers as a laminar (or quasi-laminar) flow. However, under the focusing effect caused by the VSD with a 45° diffuser, intake flow is characterized by a high level of the kinetic energy of turbulence caused by the interaction of counter-current streams. Because the convective transport of the emissions from their source to the aperture of the ventilation entrance implies no or a low

interaction with the surroundings, the application of the 45° diffuser should be rejected as the inlet device for the local ventilation operation owing to a high level of turbulence at the boundaries of the intake stream.

The above assessment was enforced by conducting direct visualization experiments on the removal of the glycerin fumes from a source located 200 mm from the

VSD. The observation of the emission catching represented here by images in Figure 8a confirms a laminar type of flow, yielding a satisfactory operation of the VSD equipped with 90° and 180° diffusers. However, the apparatus with a 45° diffuser (Figure 8b) disperses fumes outside from the upstream flow, which manifests the action of the large-scale turbulent eddies.

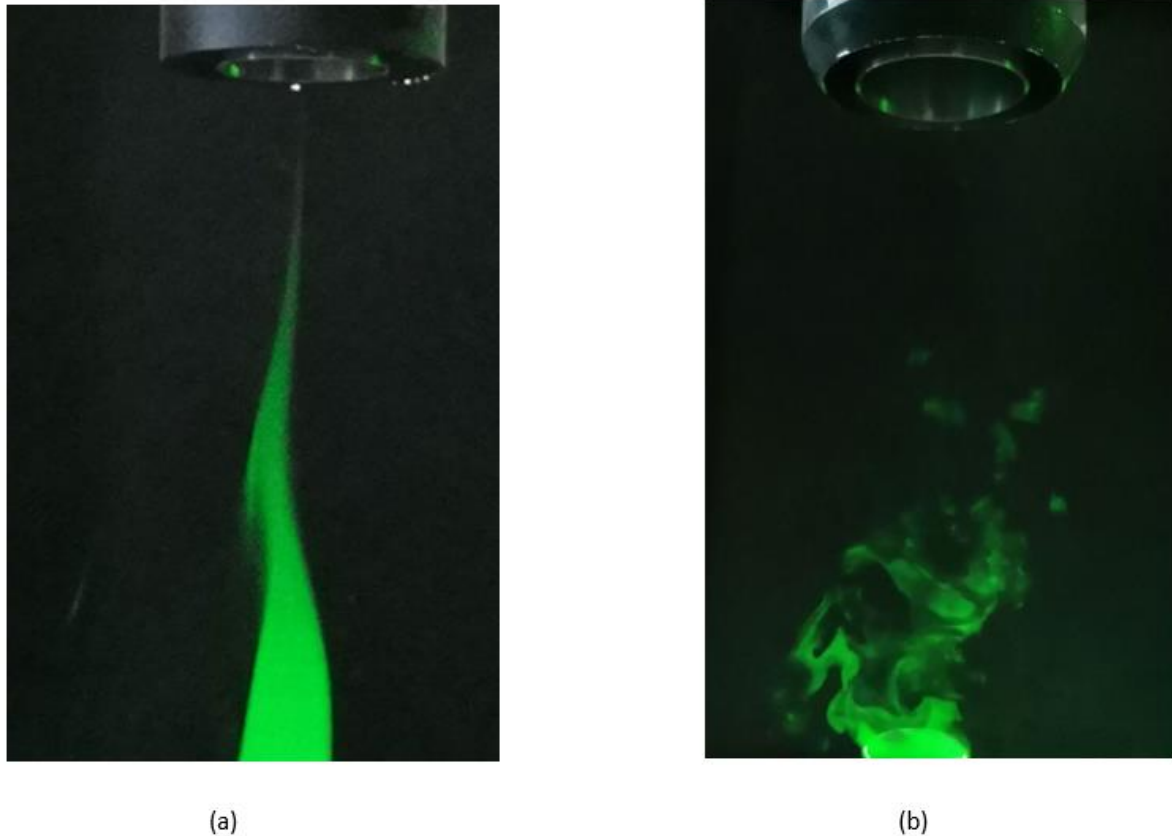


Figure 8. Visualization of the transport of the glycerin fumes by the VSD apparatuses. (a) using the VSD with a 90° diffuser, and (b) using the VSD equipped with the 45° diffuser.

Since the outcomes for the VSD with the 90° diffuser yield more interest from the point of potential application, we consider additional results from the modeling that might enlighten some specific features of the created flow configuration (further research should be conducted). For instance, the extension of the modeling space into a sphere with a diameter of 800 mm shows that the swirling jet leaving the apparatus manifests itself as a bubble skin looping the circulating cell (Figure 9a). The relevant intake-only flow streamlines are shown in Figure 9(b). Conversely, the swirling jet streamlines are presented in Figure 9(c), which demonstrates that the swirling jet does not propagate away from the VSD apparatus but is trapped in the intake flow. A comparison of the streamlines in Figure 9 indicates that a substantial part of such a complicated propagation of the swirling jet becomes the outer part of the intake flow. Therefore, the central part of the intake flow is created by the penetration of the fluid from the surrounding space into the

'favorable' laminar corridor. The associated elongation of the entrapping zone is represented by increasing the velocity values along the axis (the red line in Figure 6). The above interpretation is based on the modeling results yielded by the 2-D asymmetrical flow idealized assumption; further interest might arise in details of distortion originating from the surrounding drafts.

The operation of the VSD apparatus and the overall configuration of the induced flow field is governed by the number of parameters, such as the angular momentum flux of the peripheral flow (or the alternative swirl parameter), ratio of the mass flowrates between inflow and outflow streams, spacing ratio between the cross section areas occupied by the intake and peripheral outflowing streams, and design specification of the swirl generator and the diffuser (Spotar & Sorokin, 2010). The variation of these parameters can impact the observed focusing of the intake flow, although this confining effect comes with price - the additional shielding flow is required

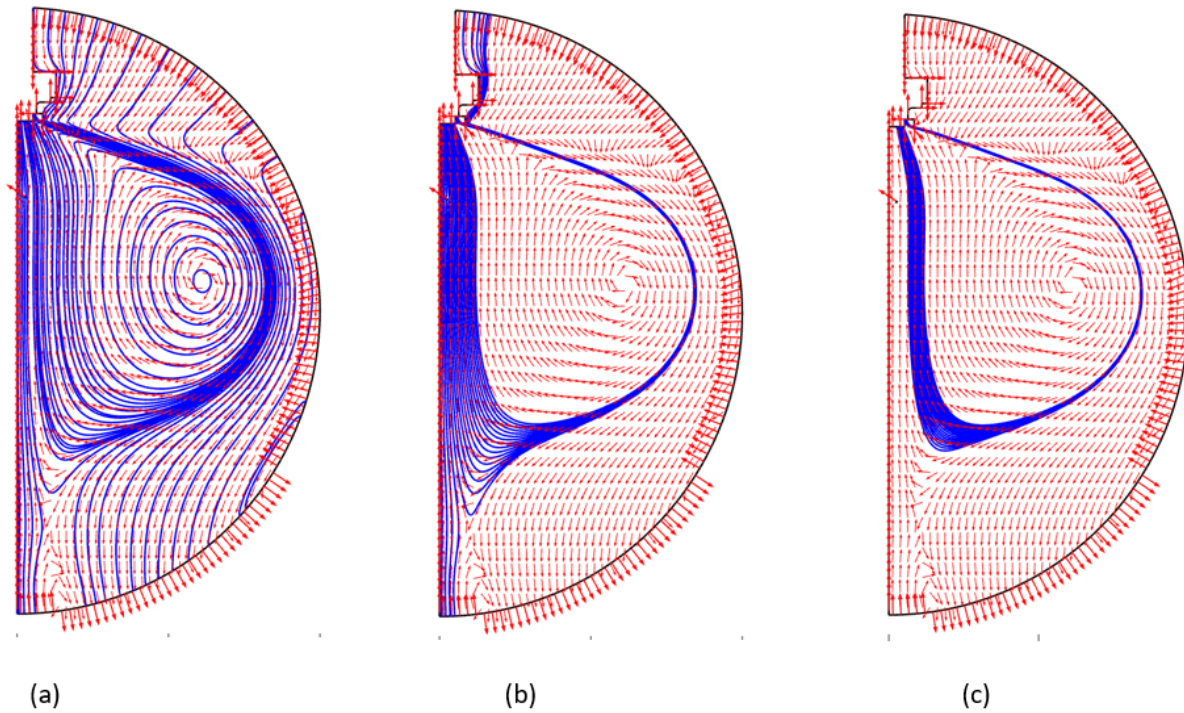
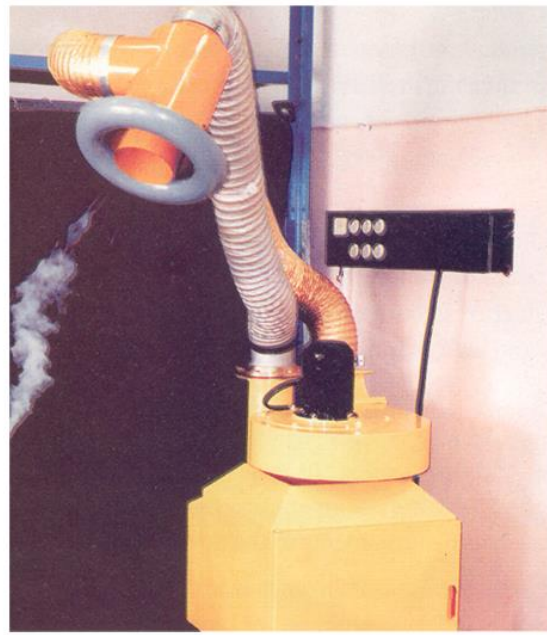


Figure 9. Configuration of the flow yielded by the VSD with $\phi = 90^\circ$ simulated in the space of 800 mm radius: (a) streamlines for the entire flow, (b) streamlines for the intake flow only, (c) streamlines for the outflowing swirling jet only.



(a)



(b)

Figure 10. (a) Application of the VSD for removal of the welding fumes, (b) fumes filtering system equipped with the VSD; (Sorokin & Spotar, 2009).

to narrow the available space for the inflow stream. In the possible applications, the geometry of the emission source should be considered, and a point-like source of emissions is the most suitable. This is because only the

central part of the intake flow is the 'undisturbed' laminar flow, and the outer region slightly interacts with the surrounding space.

The results of testing of the pilot VSD apparatuses at

an industrial scale demonstrated that the induced intake stream is more focused when compared to the suction through a standard hood and allows the removal of contaminated air at an increased positioning distance from the emission source (Figure 10, Sorokin & Spotar, 2009). However, note that, first, the described effect is associated with additional energy costs for organizing the peripheral airflow; second, the VSD apparatus is a more complex device compared to a standard ventilation intake hood. Therefore, the potential application of the described method for the problems of local ventilation is limited and opts for cases where the total positive effect may exceed the effect of these drawbacks. An obvious potential is a solution to the coordinated alignment of the supply and exhaust ventilation ducts (Martic & Zecevic, 2010). Another example is filtering ventilation units, because the additional flow serves only to concentrate the exhaust flow, thus improving the efficiency of the local ventilation system can be achieved without increasing the throughput of the filters. In addition, a filtered airflow can be used to form a peripheral swirling jet, as shown in Figure 10b, in which case the ventilation system does not require an additional ventilator.

5. Conclusions

1. The findings from CFD modeling and non-intrusive laser-Doppler anemometry diagnostics revealed the details of the confinement of the intake flow by application of the VSD apparatus.
2. The streamline's configuration and velocity profiles generated by the VSD flow crucially depend on and can be controlled by changing the geometry of the profiled diffuser conjugated with the outlet swirling jet.
3. In the possible application of the optimized VSD apparatus equipped with a 90° diffuser, a point-like source of emissions is the most favorable case. This is because only the central part of the intake flow is the 'undisturbed' laminar flow, and the outer region slightly interacts with the surrounding space.
4. The 2-D axisymmetric CFD models of the VSD operation yielded adequate compliance to the experimental velocity profiles and turbulent characteristics in the near-field region; hence, they are a convenient tool for the exploratory design of the considered ventilation task.
5. Regarding potential applications, it should be noted that to operate the VSD apparatus, an additional stream is required compared with the operation of a conventional intake hood. Therefore, the usefulness of the presented method and apparatus in handling some ventilation tasks has to be directly verified in practice. Further systematic studies are needed to investigate the correlation between the increase in the intake flow turbulence and the decrease in the diffuser opening angle (i.e., gradual smooth behavior or sharp transition).

Funding

This research was supported by the Russian Foundation for Basic Research under Grant 20-58-26003, V.I. Terekhov.

References

- Chokhar I.A. & Filippov M.V. "Local Exhaust Ventilation Suction Flare Extension Device", 2021, Russian Patent no. 2778104.
- Martic V., Zecevic N. "Kitchen Extraction Hood with Innovative Design", US2010/0126123 A1. Patent, 2010.
- Lim Y.B., Lee S.M., Lee J.W. "Characteristics of Ventilating Flow Generated by A Rotating Swirler in A Vortex Vent", *Journal of Fluids and Structures*, 27, 2011, pp. 427-437.
- Penot F., Pavlovic M.D. "Experimental Study of Non-Isothermal Diverging Swirling and Non-Swirling Annular Jets with Central Aspiration", 2010, *International Journal of Ventilation*, vol.8, issue 4, pp. 347-357.
- Shtern V., Hussain F. "Hysteresis in swirling jets". *J. Fluid. Mech*, 1996, vol.309, pp. 1-44.
- Sorokin A.L., Spotar S.Y. "Focusing of the Intake Flow for the Local Ventilation Systems", *Bulletin of Donetsk National University*, 2, 2009, pp. 118-124 (in Russian).
- Spotar S.Y., Chokhar I.A., Lukashov V.V., Prozorov D.S. "Method and Device for Local Ventilation", 1995, Russian Patent no. 2046258.
- Spotar S.Y., Sorokin A.L. "Focusing of the Flow Capture for Local Exhaust Ventilation Systems", *American Journal of Applied Sciences*, 7, 2010, pp. 732-738.
- Wan P., Feng T., and Liu R. "Characteristics Study of the Swirl Air Curtain Exhaust Hood", 2010, 4th International Conference on Bioinformatics and Biomedical Engineering. doi: 10.1109/icbbe.2010.5516594.